J. Membrane Biol. 85, 143–158 (1985)

The Journal of
Membrane Biology

Cell K Activity in Frog Skin in the Presence and Absence of Cell Current

J.F. García-Díaz, L.M. Baxendale, G. Klemperer, and A. Essig
Department of Physiology, Boston University School of Medicine, Boston, Massachusetts 02118

Summary. Cell K activity, a_K^c, was measured in the short-circuited frog skin by simultaneous cell punctures from the apical surface with open-tip and K-selective microelectrodes. Strict criteria for acceptance of impalements included constancy of the open-tip microelectrode resistance, agreement within 3% of the fractional apical voltage measured with open-tip and K-selective microelectrodes, and constancy of the differential voltage recorded between the open-tip and the K microelectrodes 30–60 sec after application of amiloride or substitution of apical Na. Skins were bathed on the serosal surface with NaCl Ringer and, to reduce paracellular Cl conductance and effects of amiloride on paracellular conductance, with $NaNO_3$ Ringer on the apical surface.

Under control conditions a_K^c was nearly constant among skins (mean ± SD = 92 ± 8 mM, 14 skins) in spite of a wide range of cellular currents (5 to 70 $\mu A/cm^2$). Cell current (and transcellular Na transport) was inhibited by either apical addition of amiloride or substitution of Na by other cations. Although in some experiments the expected small increase in a_K^c after inhibition of cell current was observed, on the average the change was not significant (98 ± 11 mM after amiloride, 101 ± 12 mM after Na substitution), even 30 min after the inhibition of cell current. The membrane potential, which in the control state ranged from −42 to −77 mV, hyperpolarized after inhibition of cell current, initially to −109 ± 5 mV, then depolarizing to a stable value (−88 ± 5 mV) after 15–25 min. At this time K was above equilibrium (E_K = 98 ± 2 mV), indicating that the active pump mechanism is still operating after inhibition of transcellular Na transport.

The measurement of a_K^c permitted the calculation of the passive K current and pump current under control conditions, assuming a "constant current source" with almost all of the basolateral conductance attributable to K. We found a significant correlation between pump current and cell current with a slope of 0.31, indicating that about one-third of the cell current is carried by the pump, i.e., a pump stoichiometry of 3Na/2K.

Key Words frog skin · anions and sodium transport · membrane potential · K activity · pump current · constant current source

Introduction

In most tight epithelia K transport is restricted to the basolateral membrane. Uptake of K is linked to the active extrusion of Na (Na-K pump) while the exit is thought to be a purely passive electrodiffusive mechanism. Microelectrode studies in frog skin (Nagel, 1979; Fisher & Helman, 1981) have shown that the basolateral membrane is almost perfectly selective to K, thus confirming the original hypothesis of Koefoed-Johnsen and Ussing (1958). While cell current through the apical membrane is carried exclusively by Na ions, the situation is less clear for the basolateral membrane. For a pump that is nonrheogenic all of the current has to be carried by K diffusing from the cell to the basolateral solution. On the other hand, if the pump is rheogenic the basolateral current will be carried by both the Na-K pump and the K diffusion pathway. Thus the question of the rheogenicity of the pump is one of central importance in epithelial electrophysiology. Measurement of the emf (the zero current potential) of the basolateral membrane immediately after inhibition of transcellular current has shown that it exceeds reasonable estimates of the K diffusion potential (Nernst potential) across this membrane (Helman, Nagel & Fisher, 1979; Nagel, 1980). This indicates that the Na-K pump contributes directly to the emf and, therefore, it carries a net current (rheogenic pump).

It is clear that accurate measurements of cell membrane potential and K activity are required for correct estimates of the K equilibrium potential and K current. Reported values of cell K activity in frog skin, both under normal conditions and after abolition of cell current, are scarce and, above all, conflicting (Nagel, García-Díaz & Armstrong, 1981; DeLong & Civan, 1983; Harvey & Kernan, 1984). In great measure this is due to the difficulties inherent in microelectrode work in this epithelium and to the poor sensitivity of the K electrode in the range of intracellular K activities (0.1 M). In the present study we simultaneously measured membrane potential and cell K activity (a_K^c) under normal trans-

porting conditions and during inhibition of transcellular current (I_c). Strict criteria were applied to validate the impalements obtained simultaneously with an open-tip and a K-selective microelectrode in two different cells. Our results show that a_K^c was essentially constant over a wide range of spontaneous I_c. Calculation of the pump current, assuming a "constant current source," indicates that it amounts to about one third of I_c. Some of these results have been published in abstract form (Baxendale, García-Díaz & Essig, 1984).

Materials and Methods

Rana pipiens pipiens obtained from either Kons (Germantown, WI) or Connecticut Valley Biological Supply Co. (Southampton, MA) were kept in an aquarium with running tap water at room temperature. Skins were mounted, outer surface up, on a perfusion chamber as previously described (Nagel, 1976; Nagel, García-Díaz & Essig, 1983*a*). Most of the experiments were performed with a chamber generously supplied by Dr. Helman (Helman & Fisher, 1977), that allows easier access from the top with two microelectrodes simultaneously. In this chamber the apical half-chamber is glued onto the skin with cyanoacrylate (Zipbond, Tescom Corp., Minneapolis, MN). With these arrangements edge damage is virtually nonexistent. A negative hydrostatic pressure of approximately 40 cm H_2O was applied to the serosal compartment to attach the skin to a supporting stainless steel grid. The serosal solution was perfused at rates of 5–10 ml/min and it could be rapidly changed by a manual noninterrupt four-way valve. The apical solution was perfused at rates of 10–20 ml/min, and changes of solutions were done with either an electrically activated solenoid three-way valve (Angar Sci. Co., Cedar Knolls, NJ, model 330) or a rotary six-way valve (Rheodyne 5011, Rainin Instrument Co., Woburn, MA). To ensure homogeneous distribution over the entire luminal surface, the perfusion fluid entered the mucosal compartment through eight fine channels located immediately above the surface of the epithelium.

At the start of the experiments both sides of the skin were perfused with NaCl Ringer of composition (in mM): NaCl 110, $CaCl_2$ 1, KOH 2.5 buffered to pH 7.8 with HEPES (3–4 mM). Usually after obtaining a stable impalement with an open-tip microelectrode the apical solution was changed to $NaNO_3$ Ringer, where all NaCl was replaced by $NaNO_3$. As described later, this reduces paracellular conductance and its response to amiloride. All control measurements of intracellular K activity (a_K^c) reported here were obtained with these bathing solutions. Na-free solutions were obtained by substituting N-methyl-D glucamine nitrate or tetramethylammonium nitrate for $NaNO_3$. In one series of experiments the skin was depolarized by perfusing the serosal bath with KCl Ringer, where KCl was substituted for NaCl. Amiloride (kindly supplied by Merck Sharp and Dohme, West Point, PA) was added to the apical solutions to a final concentration of 20 μM.

The transepithelial voltage, V_t, was measured with two calomel half cells connected by floating KCl bridges to the bathing solutions ≈0.5 mm from the tissue surfaces. Transepithelial current, I_t, was applied via two AgCl-coated Ag rings located 5 mm above or below the tissue or by two 1-M NaCl bridges connected to AgCl-coated Ag wires. The microelectrodes were connected through Ag/AgCl wires to a high impedance ($>10^{15}$ Ω) FET-input electrometer (Analog Devices, Norwood, MA models 515 J for open-tip and 515 L for ion-selective microelectrodes) with negative capacitance compensation. The resistance of the open-tip microelectrode, R_{el}, was continuously monitored using capacity coupled current injection. The skins were voltage clamped to desired values of V_t by means of an automatic clamping device (E. Nagel Biomedizinische Instrumente, Germering/Munich, FRG; *see also* Fig. 2 in Nagel et al., 1983*a*). Apical membrane potential, V_a, and V_t are referred to the apical solution. Transepithelial conductance, $g_t = -\Delta I_t/\Delta V_t$, and apical fractional voltage, $F_a = \Delta V_a/\Delta V_t$, were measured with voltage pulses $\Delta V_t = +10$ mV from the holding V_t value. The values of I_t and V_a were each obtained by means of two sample/hold amplifiers (Intersil Inc., Cupertino, CA, model IH 5110) triggered by the line frequency to sample values of I_t and V_a 2 msec immediately before the onset and before the end of the pulse. The duration of the pulse (150–400 msec) was selected in each experiment so as to obtain a steady trace of V_a in the oscilloscope after the capacitative transients had been dissipated. The voltage of the K-selective microelectrode, V_K, is also referred to the apical solution. When measuring the fractional voltage with K-selective microelectrodes, F_K, the pulse duration had to be increased to 400–500 msec due to the high impedance of these microelectrodes. The pulse frequency, usually 1 Hz, was then decreased. The values of V_a, F_a (or F_K), R_{el}, V_K (or $V_K - V_a$), I_t and g_t were recorded on a six-channel strip chart recorder (BBC-Metrawatt/Goertz, Broomfield, CO, model 460). In addition V_a, V_K and V_t (or I_t) were observed on a storage oscilloscope (Tektronix Inc., Beaverton, OR, model 5115).

Micropipettes were drawn from borosilicate glass capillary tubing with inner fibers (1.2 mm OD, WP Instruments Inc., Westhaven, CT) in a horizontal puller (Industrial Science Associates, Flushing, NY, model M-1). Open-tip microelectrodes were back filled with 1.5 M KCl and had resistances between 50 and 80 MΩ when immersed in Ringer's solution. In a series of experiments we used microelectrodes filled with 0.1 M KCl (R_{el} ≈ 200 MΩ). Potassium-selective microelectrodes were fabricated from the same glass and at the same settings of the puller used for open-tip microelectrodes. Once drawn, the micropipettes were inserted, tip upwards, in holes drilled in a Teflon stopper. Approximately 0.1 ml of Bis-(dimethylamino)-dimethylsilane (Fluka Chemical Corp., Hauppauge, NY) was added to a beaker that was closed with the stopper holding the micropipettes. This assembly was positioned inside a dessicator connected to a vacuum line, and the micropipettes were allowed to react with the silane for 2–3 min. After this they were cured on a hot plate at 250°C for 1 hr. The K exchanger resin (Corning 477315, Corning Medical, Medfield, MA) was introduced as close as possible to the tip with the help of a finely drawn glass capillary. Usually after 1 hr air bubbles disappeared from the tip, and, using a similar glass fiber, the rest of the micropipettes were filled with 0.5 M KCl.

Open tip and K-selective microelectrodes were advanced at a 15° angle with the vertical, using two separate stepping motor micromanipulators (E. Nagel Biomedizinische Instrumente, Germering/Munich, FRG, model MF-500). An impalement was first obtained with the open-tip microelectrode, and when this satisfied all criteria for acceptance (*see* Results), the K microelectrode was advanced into a different cell. On occasion the cells were punctured with the open-tip microelectrode by overcompensating for the capacitance of the input stage once the microelectrode was positioned against a cell membrane.

Calibration of K-selective microelectrodes was done in so-

lutions of pure KCl (200, 100, 50 and 10 mM) or in mixed solutions of KCl and NaCl with constant [Na] + [K] = 112.5 mM ([K] = 110, 87.5, 25 and 2.5 mM). Figure 1 shows the calibration of one of the microelectrodes used. In the range of cell K activities (≈0.1 M) it is immaterial which set of calibration solutions is used. Since the selectivity coefficient ($k_{K\text{-}Na}$) depends on the K concentration of the solutions (Edelman, Curci, Samaržija & Frömter, 1978; Armstrong & García-Díaz, 1980) a_K^c was calculated by direct interpolation from the calibration curve rather than by using the Nicolsky equation. Thus, if the regression line for the K microelectrode potential, V, *vs.* log a_K in the pure KCl solutions is

$$V = S \log a_K + i \tag{1}$$

a_K^c is calculated as

$$a_K^c = 10^{(V_K - V_o - i)/S} \tag{2}$$

where V_K and V_o are the potentials recorded with the K-selective and open-tip microelectrodes in the intracellular space, and S and i are the slope and intercept given by the regression line [Eq. (1)]. V_K, V_o and V are set to zero in the Ringer's solution. Slopes S for the K microelectrodes used in this study ranged from 57 to 60 mV/decade. For comparison purposes we calculated the selectivity coefficient for K over Na by measuring V in 0.1 M solutions of KCl and NaCl (Armstrong & García-Díaz, 1980). This ranged from 30 to 52. When a_K^c was calculated from the Nicolsky equation using $k_{K\text{-}Na}$, the values obtained overestimated the actual a_K^c, calculated with Eq. (2), by 15–26 mM. This is due to the fact that $k_{K\text{-}Na}$ measured in this way is lower than its value in Ringer (containing 2.5 mM K and 110 mM Na).

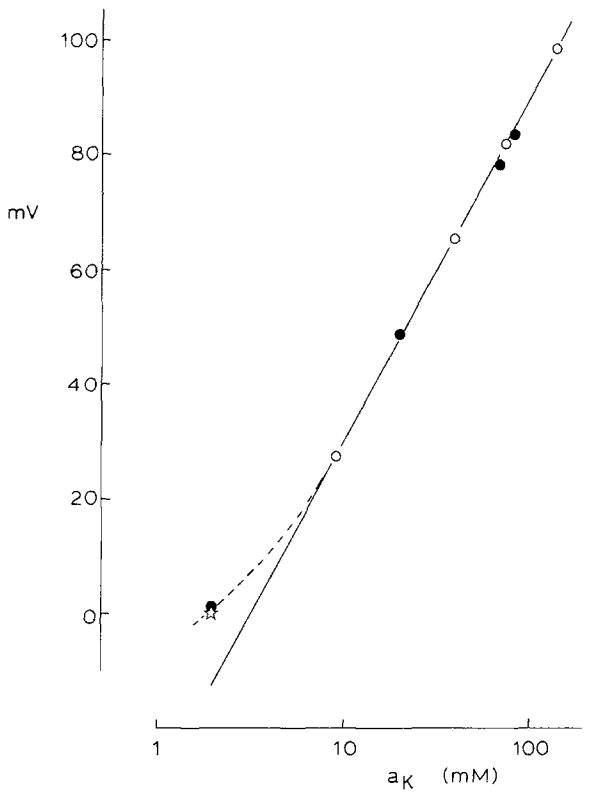

Fig. 1. Calibration curve of a K-selective microelectrode in pure KCl solutions (○) and mixed KCl-NaCl solutions (●) with [K] + [Na] = 112.5 mM. Star symbol: Ringer solution. The potential is set to zero in Ringer solution

Results

Criteria Employed to Validate Cell Punctures

Frog skin is a difficult tissue for microelectrode studies and the appearance of impalement artifacts in this and other epithelia is a well-documented phenomenon. Breaking of the microelectrode tip in crossing the cornified cell layer (stratum corneum) and subsequent damage to the membrane of the impaled cell is usually detectable by progressive depolarization of V_o and fall in F_o. A less conspicuous artifact arises when the microeletrode tip is partially occluded by cellular elements (Nelson, Ehrenfeld & Lindemann, 1978; Armstrong & García-Díaz, 1981). Figure 2 shows an example of this. After touching the epithelium, the microelectrode was first advanced in steps of 3 μm each (indicated by downward arrows). During the advance through the cornified layer R_{el} went off scale and F_o, although extremely noisy, did not indicate the crossing of a resistance barrier. At the last advance F_o increased to 0.7 and V_o jumped to a negative value, indicating cell penetration. However V_o and F_o were noisy and R_{el} was still off scale. Successive withdrawals of the microelectrode in steps of 0.5 μm (upward arrows) reduced R_{el} and decreased the noise in V_o and (eventually) in F_o. The average value of F_o did not change during withdrawal, indicating that there was not unsealing of the microelectrode. Note that at the second and third withdrawal steps V_o depolarized. These changes in V_o in association with changes in R_{el} are attributed to artifactual tip potentials (pretip potentials). Although the origin of these artifacts is not known precisely, they may arise from partial occlusion of the microelectrode tip by cellular elements. In some cases the offset in V_o is as high as 20 mV, usually negative. Even when the offset is small relative to the value of V_o, it would lead to a serious error in the calculation of a_K^c. The last backward step shown in Fig. 2 is necessary since on occasion the microelectrode tip partially breaks when crossing the stratum corneum and the actual value of R_{el} is lower than originally. Figure 2 also shows the usual responses of V_o and F_o on apical addition of amiloride. After removal of the microelectrode from the cell, one hour later, the potential in Ringer was −1 mV and R_{el} was unchanged. The insets below the F_o graph show the

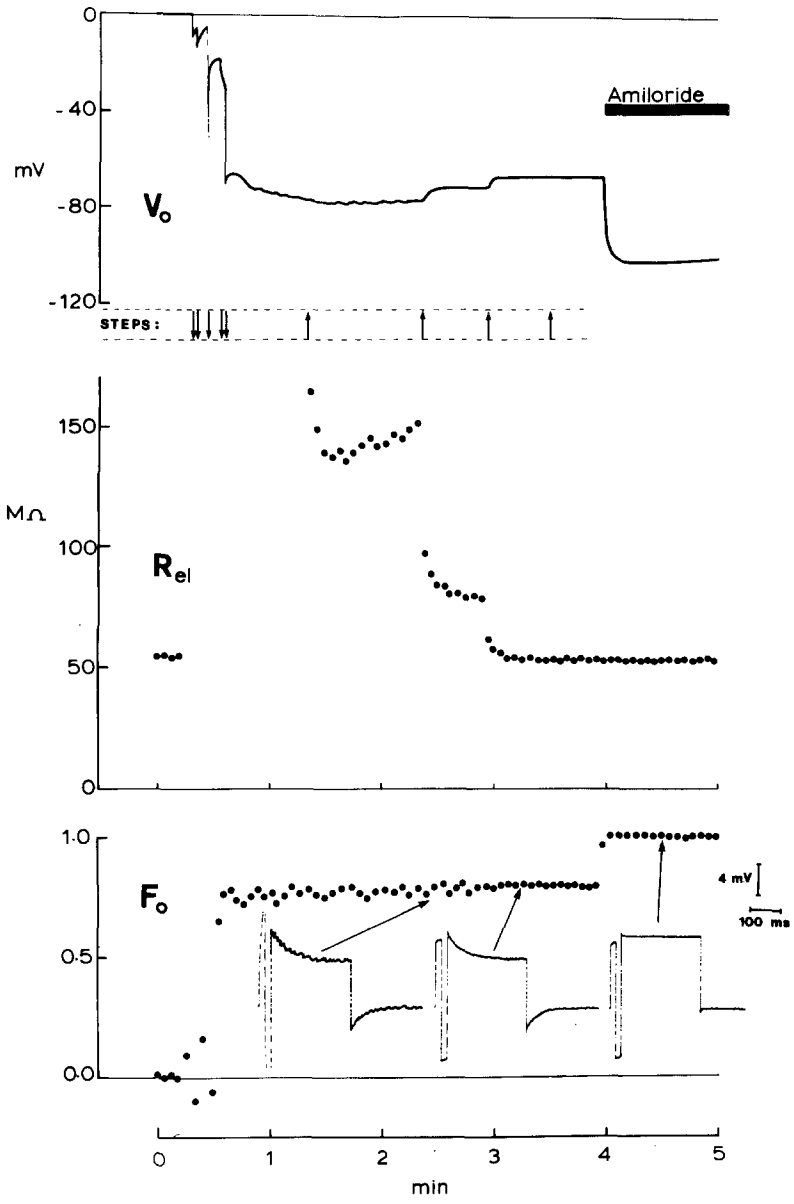

Fig. 2. Cell puncture with an open-tip microelectrode. Downward arrows indicate advancing steps of 3 μm each. Upward arrows indicate withdrawing steps of 0.5 μm each. Insets in F_o graph show oscilloscope traces of V_o responses to microelectrode current injection (to measure R_{el}) and to V_t pulse. Amiloride (20 μM) was added to the apical solution during the period marked by the bar.

oscilloscope traces of V_o during measurement of R_{el} (up and down pulses) and during application of +10 mV V_t pulses. Note that before withdrawal of the microelectrode to a position where R_{el} is close to its initial value the trace shows excessive noise and the R_{el} pulses are off scale. The middle oscilloscope trace shows an acceptable level of noise in association with a decrease of R_{el} to its initial value. In the presence of amiloride the V_o trace shows the typical square wave behavior. Other criteria for acceptance of impalements employed in these studies are as discussed elsewhere (Armstrong & García-Díaz, 1980; Nagel et al., 1981).

Some investigators have reported artifacts under certain circumstances due to KCl leakage from micropipettes filled with solutions of high concentration (Nelson et al., 1978; Fromm & Schultz, 1981; Blatt & Slayman, 1983; Stoner, Natke & Dixon, 1984). Although we have never seen evidence for this phenomenon in frog skin impalements with 1.5 M KCl filled microelectrodes of R_{el} > 30 MΩ, we performed some experiments where the same skin was consecutively impaled with either 1.5 or 0.1 M KCl filled micropipettes. The lower KCl concentration is close to the expected cellular K concentration, and thus we presume that any leakage will be minimal. We did not find any difference in the stability of the recordings or in the response to the addition of mucosal amiloride between impalements obtained with either of these microelectrodes. Table 1 lists the values of V_o and F_o for four experiments. The only significant differ-

Table 1. Membrane potential and apical fractional voltage measured with 1.5 and 0.1 M KCl-filled microelectrodes in short-circuited frog skin

Exp. No.	Filling solution						ΔV_o (mV)	ΔF_o
	1.5 M KCl			0.1 M KCl				
	V_o (mV)	F_o	R_{el} (MΩ)	V_o (mV)	F_o	R_{el} (MΩ)		
1	−76	0.83	50	−72	0.83	175	4	0.00
2	−68	0.78	75	−61	0.67	180	7	−0.11
3	−57	0.67	68	−49	0.60	180	8	−0.07
4	−40	0.60	50	−37	0.62	200	3	0.02
Mean							5.5	−0.05
SD							2.4	0.05

ence was a less negative value of V_o obtained with the 0.1 M microelectrodes. In part this is due to a change in the junction potential at the tip of the 0.1 M microelectrode when it is advanced from the $NaNO_3$ Ringer into the intracellular space. If, in a simplistic approach, we assume the intracellular space to be a 0.1 M KCl solution, the measured change in junction potential is 2.5 mV. Thus the actual V_o's are only 0.5–5.5 mV more positive when measured with the 0.1 M microelectrodes. We take the values recorded with the 1.5 M microelectrodes as more accurate measurements of the actual V_o, since these are less affected by junction potentials.

As explained above, continuous monitoring of R_{el} is essential for the correct measurement of V_o. However, it is not possible to record the resistance of the ion-selective microelectrodes as rapidly as needed for the assessment of proper intracellular location of the tip. Thus other criteria had to be established for this purpose. With this aim, we measured V_o simultaneously with two open-tip microelectrodes in several skins. To simulate the experimental situation to be found when measuring a^c_K, only R_{el} of one of the open-tip microelectrodes was recorded. Figure 3 shows one of these experiments. The upper record shows the difference in V_o recorded by the two microelectrodes, $V_o(1) - V_o(2)$. R_{el} was continuously measured only with electrode 2 (not shown). On application of 20 μM amiloride or removal of apical Na, V_o hyperpolarized by some 70 mV and F_o increased to ≈1.0. About 20–30 sec after application of amiloride and the removal of Na, $V_o(1) - V_o(2)$ was 2 and 4 mV, respectively. The fast initial transients in this trace, as well as the slower one observed after removal of amiloride, are due to unequal mixing of solutions at the different locations of the microelectrodes in the chamber, in spite of the fast perfusion rate and the homogeneous arrangement of the perfusion inlets. The magnitude

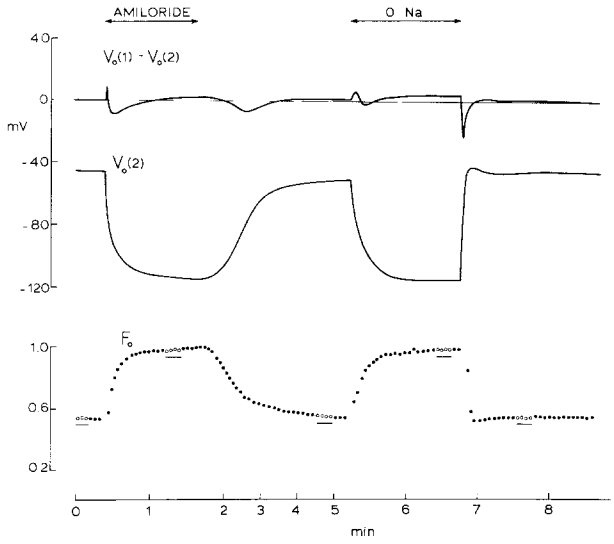

Fig. 3. Simultaneous measurement of V_o with two open-tip microelectrodes. $V_o(1) - V_o(2)$ is the differential output of the two electrodes. At the times indicated amiloride (20 μM) was added to the apical solution or N-methyl-D-glucamine was substituted for Na. F_o was measured with electrode 2 except for the periods marked by the bars and open circles where it was measured with electrode 1.

and direction of the transients depended on the relative position of the microelectrodes. The cells in the center of the chamber respond faster to alterations in solution composition. On returning to control solutions all variables assumed their original values. During the periods where the F_o trace is underlined by bars (open circles) this variable was measured with electrode (1). No difference was found in these experiments between the F_o measured with either electrode, under control conditions or during inhibition of cell current. We do not ascribe any special significance to the change in $V_o(1) - V_o(2)$ (2–4 mV) seen between the control state and after inhibi-

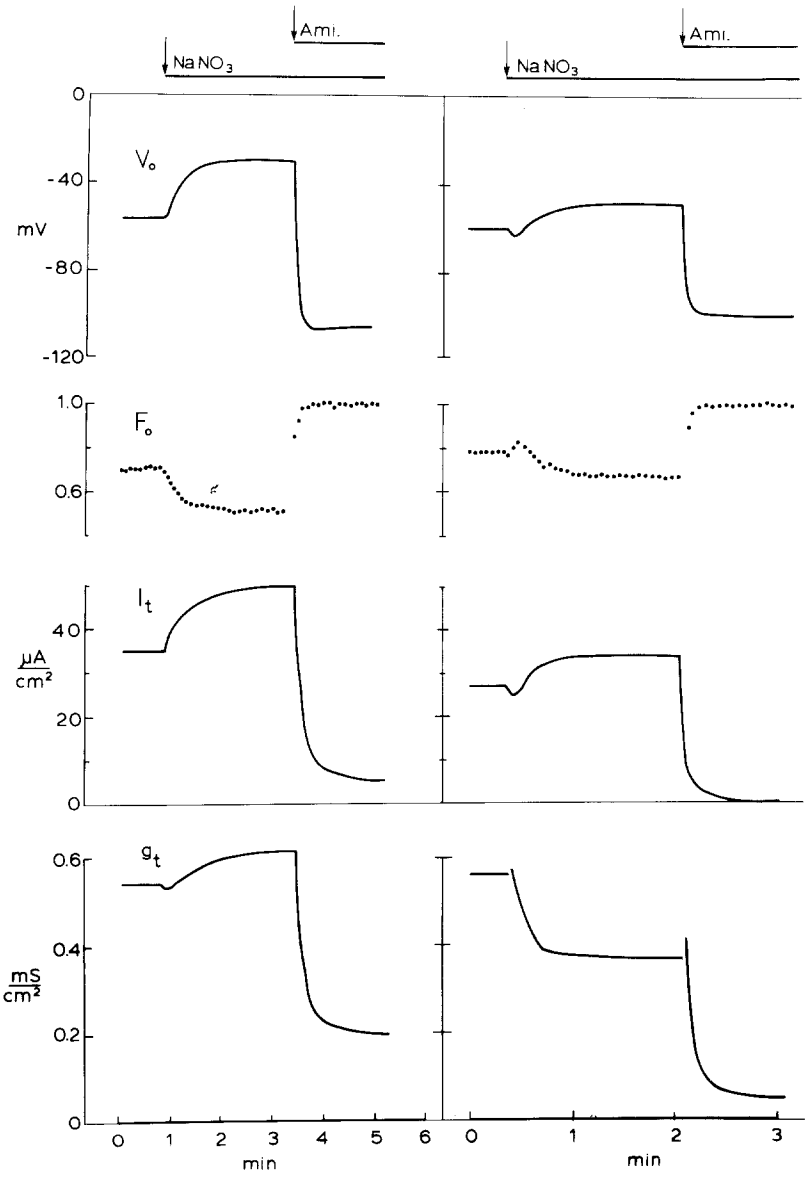

Fig. 4. Effects of apical substitution of NO_3 for Cl in two different skins. The skin of the right panel clearly shows a paracellular Cl conductance ("leaky" skin). Amiloride (20 μM) was added to the apical solution at the times indicated

tion of cell current, other than the limit of accuracy of this technique. In most of the experiments the change in $V_o(1) - V_o(2)$ was <2 mV and the F_o measured with both electrodes agreed within 3%. There were, however, cases where $V_o(1) - V_o(2)$ changed as much as 15 mV, usually associated with recordings with large differences in the F_o values measured with the two electrodes during the control period. These were taken to be artifacts, although no instability or noise was apparent in the recordings. Accordingly, we applied the following criteria to accept simultaneous cell punctures. Once a satisfactory impalement was obtained with an open-tip microelectrode, the K-selective microelectrode was advanced into the epithelium and a cell puncture accepted if the F_o measured with both electrodes agreed within 3% and if, after inhibition of cell current (either by addition of amiloride or removal of external Na), $V_K - V_o$ changed by <2 mV immediately after the initial fast transient (lasting <30 sec).

Effects of Apical Cl Substitution on the Electrophysiology of Frog Skin

In an earlier study (Nagel, García-Díaz & Essig, 1983*b*) we found that in skins with large paracellular conductance the apical fractional resistance $R_o/(R_o + R_i)$ (where R_o and R_i are the lumped equivalent resistances of the apical and basolateral membranes, respectively) is underestimated by F_o $(=\Delta V_o/\Delta V_t)$. It was also found that the conven-

tional method of determining cell conductance, g_c, by application of amiloride leads to erroneous values when used in large conductance skins, since there is an effect of amiloride on paracellular conductance (possibly secondary to the inhibition of cellular Na transport). These complications are greatly reduced by substitution of apical Cl by other anions (Nagel et al., 1983*a*,*b*). Consequently, we performed these experiments in skins bathed on the apical surface by $NaNO_3$ Ringer ([Cl] = 2 mM). Figure 4 shows the two major effects induced by the substitution of NO_3 for Cl on the electrophysiology of frog skin. In the experiment at the left all the changes in variables (increases in I_t and g_t, depolarization of V_o, decrease in F_o) indicate a stimulation of apical Na entry mediated by an increased apical conductance. This was confirmed by application of amiloride before and after the Cl substitution. In the experiment shown at the right in Fig. 4 there is also stimulation of Na transport, although to a lesser degree (increase in I_t, depolarization of V_o and decrease in F_o), but g_t *decreased*. Application of amiloride before and after Cl substitution showed that this decrease of g_t is of paracellular origin. Skins with this behavior were termed "leaky" and were most often found during the months of April–October. Substitution of Cl by NO_3, gluconate or methylsulphate always induced the same reversible decrease in g_t in "leaky" frogs, although gluconate and methylsulphate either slightly inhibited Na transport or did not affect it at all. Thus, removal of apical Cl exerts two different effects on frog skin. One is a decrease in paracellular conductance independent of the anion used for substitution. In addition the anion composition of the apical solution has a direct effect on apical Na entry.

As already mentioned, addition of mucosal amiloride in NaCl Ringer induces a secondary reduction in paracellular conductance in "leaky" frogs. This is usually seen as a slow decrease in g_t after the initial fast inhibition (Nagel et al., 1983*b*). On the other hand, in skins with the apical surface bathed in Cl-free Ringer, application of 20 μM amiloride induces only a fast decrease in g_t in most of the experiments.[1] This allows a more accurate evaluations of the cellular conductance, g_c. The amiloride dose employed in these experiments (20 μM) reduced I_t at short circuit to a mean value of 1.5 ± 1.4 $\mu A/cm^2$. Higher doses did not reduce I_t any further. This residual current is not due to paracellular back flux of Cl since it was the same when the tissue was bathed on both sides with identical NaCl Ringer solutions. The relationship of cell current and conductance (defined respectively as the amiloride inhibitable portion of I_t and g_t) under short-circuit conditions is plotted in Fig. 5 for the 14 skins used in these experiments (Table 2). As shown in this figure, there was a good linear correlation between these variables. The slope, 97.2 mV, is the cell Thévenin emf, which seems to be approximately constant for all the skins studied.[2]

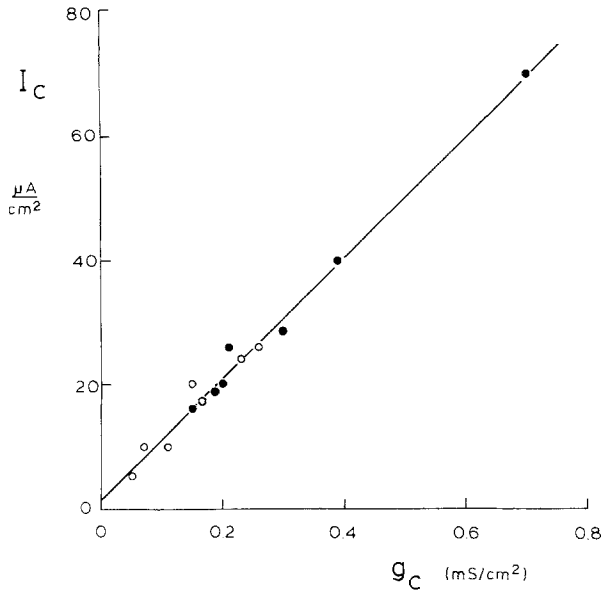

Fig. 5. Relation between cell current and conductance at short circuit for the 14 frogs studied, bathed with $NaNO_3$ Ringer at the apical surface. Open circles represent "leaky" skins, i.e., their behavior after substituting NO_3 for Cl is that shown in the right panel of Fig. 4. The regression line was $I_c = 97.2\ g_c + 1.6$, $r = 0.99$ ($P < 0.001$)

Cell K Activity in the Control State and After Inhibition of Cell Current

All measurements of cell K activity were done by simultaneously recording V_K and V_o. Figure 6 shows one of the experiments. The second trace is the difference $V_K - V_o$, which is directly related to a_K^c [Eq. (2)]. Under control conditions $V_K - V_o$ in this experiment was 85 mV, which on calibration of the K-selective microelectrode corresponded to an a_K^c of 102 mM. Application of apical amiloride elic-

[1] However, note in Fig. 6 the secondary and slower decrease in g_t (at min 3) after addition of amiloride, in spite of bathing the apical surface with $NaNO_3$ Ringer. These secondary decreases were observed on occasion, but they were temporally separated from the initial fast decrease of g_t, so that evaluation of g_c was always possible.

[2] There were also in these experiments positive correlations between I_c and each of the cell membrane conductances. The significance of these findings is presently under investigation.

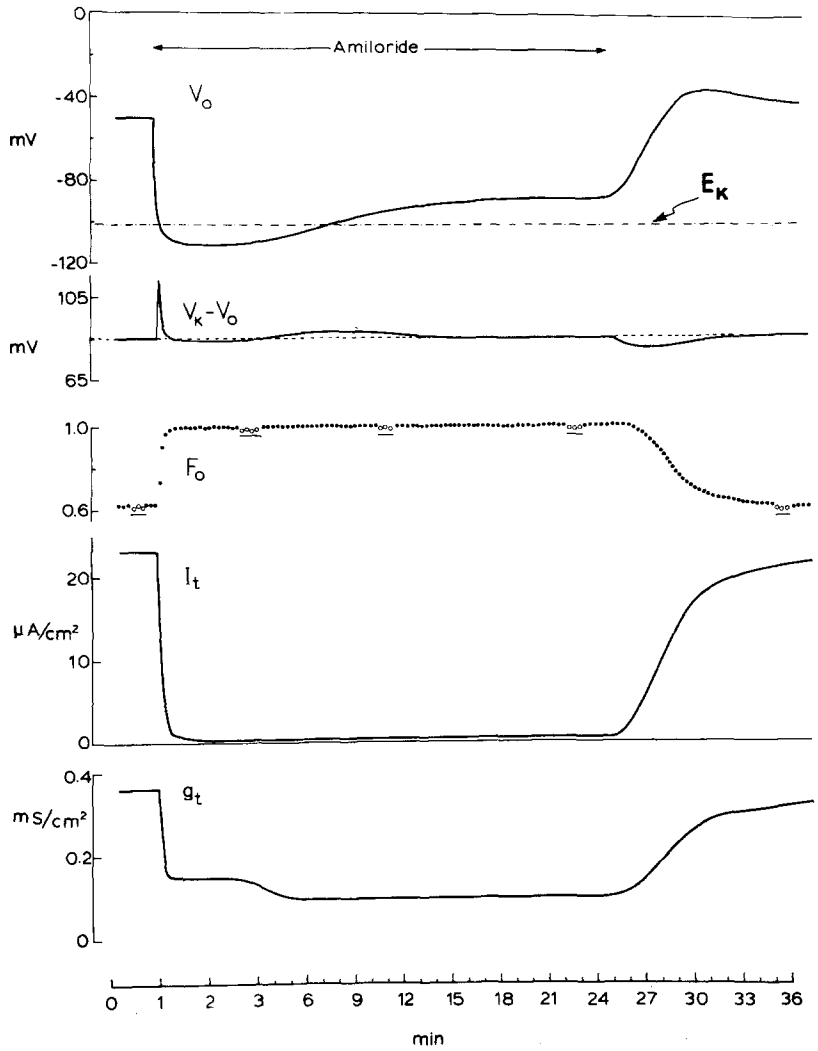

Fig. 6. Simultaneous recording of V_o and V_K during addition of amiloride (20 μM). $V_K - V_o$ is the differential output of the voltages recorded with the open-tip and the K-selective microelectrodes. F_o was measured with the open-tip microelectrode except during the periods marked by the bars and open circles where it was measured with the K electrode. E_K is the calculated K equilibrium potential for this experiment. Note change of time scale at min 3

ited the usual changes in V_o, F_o, I_t and g_t. Immediately after the amiloride addition there was a fast transient in $V_K - V_o$. As shown previously in the experiments with two open-tip microelectrodes (Fig. 3), this transient is due to unequal mixing of solutions in different regions of the apical compartment. After this fast transient, $V_K - V_o$ slowly oscillated around the initial value. These oscillations, usually less than 4 mV, were associated with changes in V_o, as were the initial and final transients during addition and removal of amiloride. In the steady state after addition of the drug, i.e., once V_o reached a stable value, usually in 15–25 min, $V_K - V_o$ remained at the initial value. Removal of amiloride also induced a transient in $V_K - V_o$, slower than the one seen after addition and also due to lack of synchronization of the different cells. Table 2 lists all the experiments of this type performed. Although in some skins a change in a_K^c after amiloride was observed, this was not consistent. The mean values in the control state and after the addition of amiloride were not significantly different ($P > 0.4$). As shown in Table 2, $V_K - V_o$ (and thus a_K^c) varied only slightly in spite of appreciable variability of V_o and V_K among the individual skins. Thus, although in general skins with high I_c had lower V_o, there was no correlation between a_K^c and I_c or V_o.

The behavior shown by V_o in Fig. 6 was typical of all of these experiments. There was an initial hyperpolarization of V_i ($=-V_o$) to a value, E_i^{max}, larger than the K equilibrium potential across the basolateral membrane, E_K (calculated from the Nernst equation and the measured a_K^c), after which V_i slowly depolarized to a steady-state value, E_i^{∞}, smaller than E_K. Table 2 shows that, on the average, E_i^{max} exceeds E_K by 11 mV ($P < 0.05$) and that E_i^{∞} is 10 mV smaller than E_K ($P < 0.05$).[3]

[3] Since the skins are short circuited, $V_o = -V_i$. V_i obeys the relation $V_i = E_i - I_c R_i$, where E_i is the emf (zero current potential) of the basolateral (inner) membrane, R_i its lumped equivalent resistance, and I_c the cell current. After amiloride $I_c = 0$ and then $V_o = -V_i = -E_i$. Thus the values of V_i in the presence of amiloride in Table 2 (columns 8 and 9) have been named E_i^{max} and E_i^{∞}.

Table 2. Cell current, membrane potential and cell K activity in short-circuited frog skin: Effects of amiloride

Skin	I_t (μA/cm^2)	V_o (mV)	V_K (mV)	$V_K - V_o$ (mV)	a_K^c (mM)	a_K^c(Amil.) (mM)	E_i^{max} (mV)	E_i^x (mV)	E_K (mV)
1	20	−72	13	85	93	105	110	—	99
2	10	−77	9	86	85	100	108	—	96
3	24	−74	13	87	91	91	110	99	98
4	70	−45	41	86	90	93	122	92	98
5	26	−52	33	85	102	102	112	89	101
6	40	−55	34	89	83	77	111	90	96
7	20	−67	11	78	89	93	108	80	98
8	10	−56	30	86	86	86	106	88	97
9	15	−74	9	83	83	87	104	89	96
10	5	−68	18	86	88	107	100	88	97
11	26	−68	16	84	88	92	106	85	97
12	17	−58	22	80	102	110	111	86	101
13	19	−42	42	84	101	118	113	83	101
14	28	−48	40	88	105	105	111	92	102
Mean				85	92	98	109	88	98
SD				3	8	11	5	5	2

E_i^{max} and E_i^x are the peak hyperpolarization and the steady-state value of V_i ($=-V_o$) after apical addition of amiloride (20 μM). E_K is the K equilibrium potential.

Table 3. Transepithelial current, membrane potential and cell K activity in short-circuited frog skin: Effects of apical Na substitution

Expt.	$[Na]_o$ = 110 mM				$[Na]_o$ = 0			
	I_t (μA/cm^2)	V_o (mV)	$V_K - V_o$ (mV)	a_K^c (mM)	I_t (μA/cm^2)	V_o (mV)	$V_K - V_o$ (mV)	a_K^c (mM)
a	21.5	−65	84	89	−2.5	−109	88	104
b	22.5	−60	84	89	0.0	−109	88	104
c	68.5	−46	86	90	1.0	−121	86	90
d	22.0	−53	83	94	−1.0	−110	83	94
e	17.0	−77	82	83	−2.0	−100	83	87
f	5.0	−71	88	95	−1.0	−92	91	107
g	28.0	−67	84	88	−2.0	−110	84	88
h	18.5	−50	86	110	−1.0	−118	90	126
i	35.0	−60	86	97	0.5	−115	88	105
Mean			85	93	−1.0	−109	87	101
SD			2	8	1.2	9	3	12

Values in 0 Na are taken at the quasi-steady state, 2–5 min after substitution. Experiments a and b are from the same skin. In b tetramethylammonium was substituted for apical Na. In all others N-methyl-D-glucamine was used.

In several experiments cell current was abolished by substitution of N-methyl-D-glucamine (NMDG) or tetramethylammonium (TMA) for apical Na. Figure 7 shows an experiment done in the same skin as the one shown in Fig. 6. Removal of Na elicited the same changes in all variables as the addition of amiloride, i.e., hyperpolarization of V_o, decreases in I_t and g_t (not shown) and increase in F_o to 1.0 (not shown). $V_K - V_o$ remained constant after an initial transient. On restoring Na, V_o depolarized rapidly and then slowly repolarized towards the initial value. Again, $V_K - V_o$ returned to control values after a transient. As shown in Fig. 7, the behavior of V_o was exactly the same as after addition of amiloride (Fig. 7). In each individual experiment the peak hyperpolarization, E_i^{max}, was the same after addition of amiloride or Na substitution.

The results of nine experiments with mucosal Na substitutions are listed in Table 3. Although in individual experiments a_K^c either increased or remained constant after removal of Na, the difference, 8 ± 7 mM, was not significant ($P > 0.2$). I_t

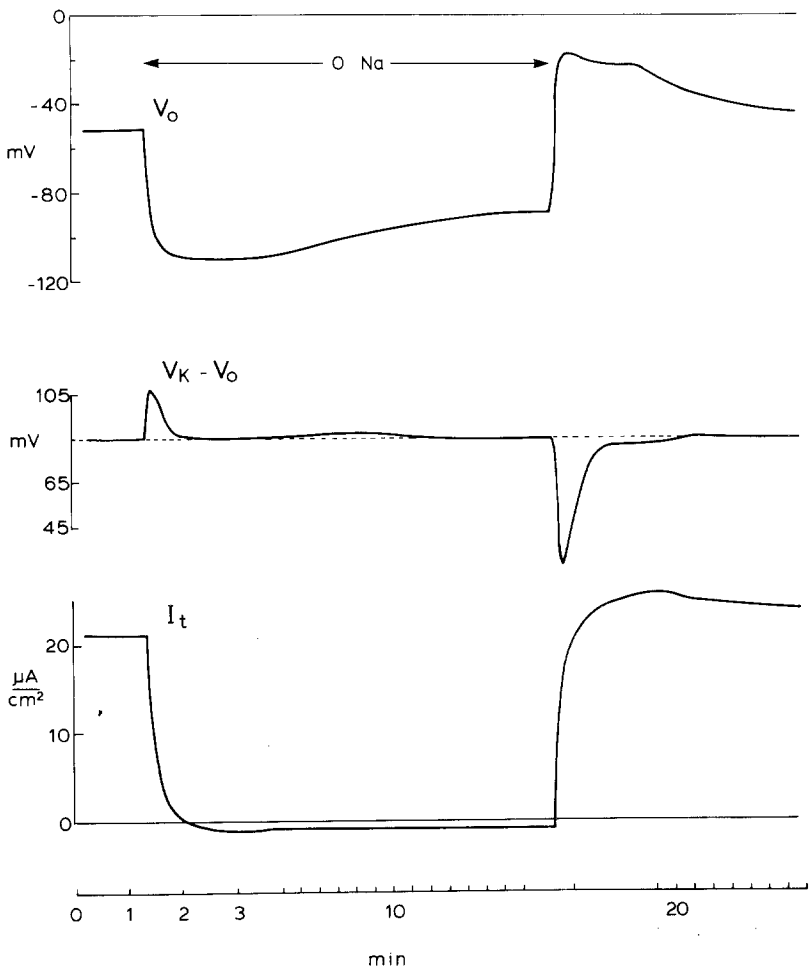

Fig. 7. Simultaneous recording of V_o and V_K during apical substitution of N-methyl-D-glucamine for Na. Note that the recorder speed is increased during removal and restoration of Na

assumed slightly negative values after substitution of NMDG for Na. The difference in I_t values following amiloride addition and substitution of NMDG for Na (2.5 μA/cm^2) probably reflects a small paracellular backflux (serosa to mucosa) of Na.

Membrane Depolarization with High Serosa K

If the basolateral membrane of frog skin exhibited almost exclusive permeability to K, increasing the serosal K activity to a value close to the measured a_K^c should almost completely depolarize the basolateral emf, E_i, since any contribution to E_i from the pump would be shunted by the increased K conductance. By replacing all serosal Na by K, the serosal K activity is increased to 87 mM. Since the mean a_K^c measured in these experiments was 92 mM (Table 2) one would expect E_i to be 2 mV (cell negative) after this substitution. Figure 8 and Table 4 show the results of some experiments where the above assumption was tested. In Fig. 8 serosal substitution of K for Na depolarized V_o from −90 to 0 mV in about 8 min. Addition of apical amiloride to inhibit cell current slightly hyperpolarized V_o, to −2 mV. (Under these conditions $E_i = -V_o$; *see* footnote 2). Four experiments like the one shown in Fig. 8 are listed in Table 4 (1 to 4). Since during the time needed to depolarize the basolateral membrane, before the addition of amiloride, a_K^c could have changed due to the increased serosal K activity, we performed three more experiments where mucosal amiloride was first added and then serosal K was substituted for Na. This second series is also shown in Table 4 (experiments 5 to 7). Addition of amiloride induced the typical hyperpolarization of V_o. Subsequent increase of serosal K depolarized V_o in about 2 to 5 min to values between 0 and −5 mV (mean ± SD = −2 ± 3). Therefore these results are consistent with the measured values of a_K^c.

Figure 8 also shows an increase in F_o after inner substitution of K for Na, which is due to an increased basolateral conductance. The increase in g_t under these conditions has been also observed by other investigators (Ussing, Biber & Bricker, 1965;

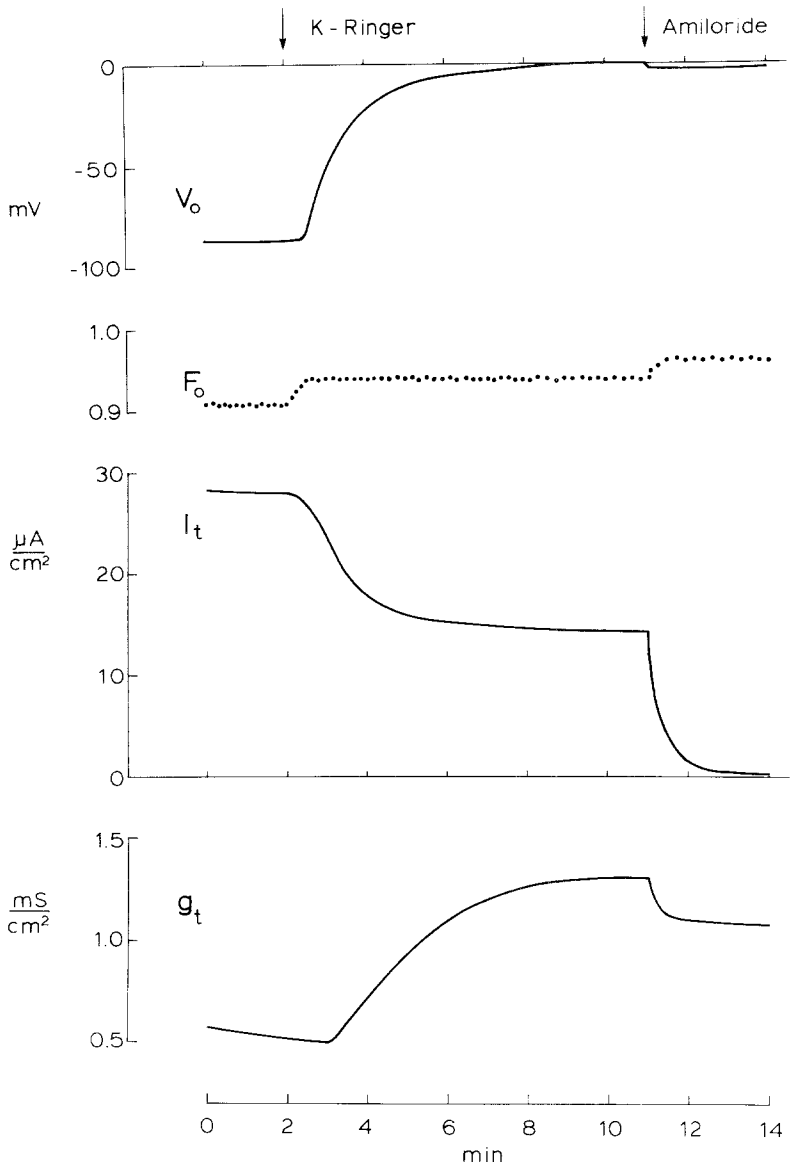

Fig. 8. Depolarization of V_o by high serosa K in short-circuited frog skin. At the first arrow K was substituted for Na at the inner solution. At the second arrow 20 μM amiloride was added to the apical solution

Fuchs, Larsen & Lindemann, 1977) and is mainly due to a large increase in paracellular conductance (note the high residual g_t after amiloride). Addition of amiloride showed that the decrease in I_t is due to a decreased cell current, since subsequent to addition of amiloride I_t became zero. Rick et al. (1984) also observed this decrease in cell current after inner substitution of choline for Na and showed that it is due to uncoupling of the cells after removal of inner Na.

Estimates of Basolateral K and Pump Currents

The equivalent electrical circuit for the basolateral membrane of frog skin is assumed to consist of two parallel pathways: a purely diffusive K pathway and a pump pathway (Koefoed-Johnsen & Ussing, 1958; Lindemann, 1977; Nagel, 1980). The K-diffusive current is given by

$$I_K^d = g_K(E_K - V_i) \tag{3}$$

where g_K and E_K are the conductance and equilibrium potential for K. The pump is often assumed to behave as a constant current generator, i.e., its intrinsic conductance is much smaller than g_K (Lindemann, 1977; Nagel, 1980). Thus $g_K \simeq g_i$. Previous observations (*see* Discussion) indicate that when the basolateral membrane potential is altered g_i remains constant. Then g_i can be estimated by simply altering the cell current (e.g., after inhibition by amiloride) and observing the change in V_i, i.e.,

Table 4. Membrane potential depolarization by high serosa K in the presence and absence of cell current in short-circuited frog skin

Skin	NaCl Ringer	KCl Ringer	KCl Ringer + amiloride
1	−90	0	−2
2	−70	−3	−4
3	−73	0	−2
4	−78	−6	−15
Mean		−2	−6
SD		2	8
Skin	NaCl Ringer	NaCl Ringer + amiloride	KCl Ringer + amiloride
5	−70	−103	−5
6	−100	−113	−2
7	−50	−114	0
Mean		−110	−2
SD		6	3

V_o values in mV. KCl Ringer was substituted for NaCl Ringer in the serosal bath only. Amiloride (20 μM) was added to the apical solution.

$$g_i = -\frac{\Delta I_c}{\Delta V_i} = \frac{I_c}{E_i^{max} - V_i}. \quad (4)$$

It is then possible to calculate I_K^d from Eq. (3), since V_i (here equal to $-V_o$), E_K and g_K ($=g_i$) are all known for the experiments in Table 2. Since

$$I_c = I_K^d + I_p \quad (5)$$

the pump current, I_p, can also be estimated for each of these experiments. Table 5 lists the values obtained for g_i, I_K^d and I_p together with the measured I_c. As shown in Fig. 9, there is a significant correlation between I_p and I_c. The slope of the regression line, 0.31, indicates that about one-third of the basolateral or cell current is carried by the pump. This implies a stoichiometry of 3Na/2K for the pump.

Table 5. Cell current, basolateral conductance and K and pump currents in short-circuited frog skin

Skin	I_c (μA/cm²)	g_i (mS/cm²)	I_K^d (μA/cm²)	I_p (μA/cm²)
1	20	0.53	14.2	5.8
2	10	0.32	6.1	3.9
3	24	0.67	16.0	8.0
4	70	0.91	48.2	21.8
5	26	0.43	21.2	4.8
6	40	0.71	29.3	10.7
7	20	0.49	15.1	4.9
8	10	0.20	8.2	1.8
9	15	0.50	11.0	4.0
10	5	0.16	4.5	0.5
11	26	0.68	19.9	6.1
12	17	0.32	13.8	3.2
13	19	0.27	15.8	3.2
14	28	0.44	24.0	4.0

Discussion

Electrophysiology of Frog Skin

In the present study a_K^c and other electrophysiological variables of frog skin were measured with $NaNO_3$ Ringer as the apical solution. The advantage of this approach is that it allows a more accurate measurement of F_o and g_c than in NaCl Ringer, especially in skins with large paracellular conductance (Nagel et al., 1983*a*,*b*). As shown in Results, substitution of NO_3 for Cl has two different effects on the electrophysiology of frog skin. One is a simulation of Na entry mediated by an increased apical conductance. Substitution of gluconate or methylsulphate for Cl, however, either slightly depressed Na transport or did not affect it. Several investigators have reported on the effects of anions on Na transport in tight epithelia (Singer & Civan, 1971; Turnheim, Frizzell & Schultz, 1977). However, the specific mechanism by which anions affect apical Na conductance is unknown. In our experiments the stimulation of I_c by NO_3 was highly variable among skins, ranging from less than 5% to about 60%.

The other common effect of apical Cl replacement in frog skin is a decrease in paracellular conductance. This effect is induced by all anions used to substitute for Cl. The influence of Cl is particularly relevant in the determination of g_c by addition of amiloride. We found that when the apical solution is NaCl Ringer, addition of amiloride may induce an initial fast decrease in g_t followed by a much slower decrease due to a reduction of paracellular conductance (Nagel et al., 1983*b*). In most cases the two effects start simultaneously, making the determination of g_c extremely difficult. The dependence of g_t on the apical Cl concentration and the secondary effects of amiloride on g_t have also been observed by Kristensen (1983, Figs. 1 and 9). Our observations are consistent with the existence of a significant paracellular conductance to Cl when this ion is present in the apical solution. They do not, however, support the notion of a mechanism for Cl transport at the apical membrane, as suggested by Kristensen (1983).

Recently Nielsen (1984) has reported the pres-

ence of an apical Ba-inhibitable outward flux of K in skins of European frogs, *R. temporaria*, bathed in symmetrical gluconate Ringer's solutions. Our observations do not indicate the presence of such a mechanism in *R. pipiens* bathed with gluconate or NO_3 Ringer's at the apical surface alone. Under these conditions addition of amiloride decreased I_t to a mean value of 1.5 $\mu A/cm^2$ (opposite in direction to the K current found by Nielsen). In some experiments we added Ba (5 mM) or tetraethylammonium (10 mM) to the apical solution (in addition to amiloride) without any effect on the remaining I_t. As mentioned in Results, this residual current is unlikely to result from paracellular backflux of Cl since it was the same when the tissue was bathed by symmetrical NaCl solutions. It may represent an amiloride-insensitive Na flux or a Cl secretion by the gland cells (Thompson & Mills, 1983).

The slope of the regression line in Fig. 5, $\Delta I_c/\Delta g_c$, is the Thévenin equivalent cell emf, E_c. A simple linear circuit analysis shows that $E_c = E_o + E_i$, where E_o and E_i are the emf of the apical and basolateral membranes, respectively. Since $E_c = 97$ mV and $E_i = 109$ mV (Table 2), we obtain $E_o = -12$ mV. As Helman and Thompson (1982) have clearly pointed out, this E_o is a Thévenin equivalent emf for the apical membrane and cannot be identified with the reversal potential for this membrane. This discrepancy arises from the highly nonlinear behavior of the *I-V* relationship of the apical membrane (Fisher & Helman, 1981; Helman & Thompson, 1982). A different situation applies to the basolateral membrane, where such striking nonlinearity is not observed (*see* below). Thus E_i is both a Thévenin equivalent and the reversal potential for the basolateral membrane (which includes the contribution of both the K chemical potential and the pump). Preliminary measurements of a^c_{Na} in our laboratory give an estimate of the Na equilibrium potential of about +60 mV. Inasmuch as this is the only ion transported across the apical membrane, one can estimate the cell reversal potential as 60 + 109 = 169 mV, in good agreement with recent direct measurements: 165 mV (Nagel et al., 1983*c*).

Cell K Activity

Accurate measurement of a^c_K in epithelia, particularly in frog skin, requires the use of strict validation criteria for cell punctures. As we show in this study (Fig. 2), control of R_{el} is of major importance in this respect. Otherwise, recordings of V_o can be affected by artifacts of up to 20 mV. This would introduce a serious error in the estimate of a^c_K since in the range 0.1 M the sensitivity of an ion-selective

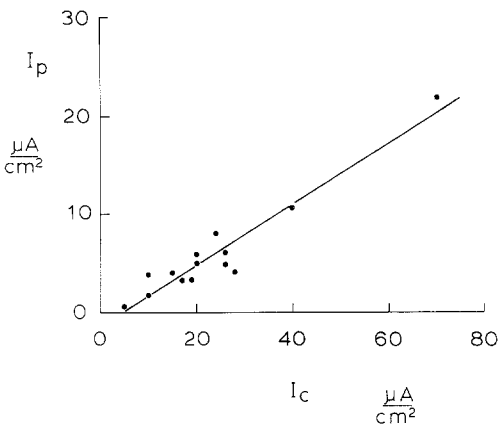

Fig. 9. Relation between cell current and pump current at short circuit. *See* text for details on the calculation of I_p. Regression line: $I_p = 0.31 \cdot I_c - 1.5$; $r = 0.96$ ($P < 0.001$). The intercept does not differ significantly from the origin ($P > 0.05$). The slope does not differ significantly from 0.33 ($P > 0.6$) and does differ from 0.50 ($P < 0.001$)

electrode is roughly 4 mM for each mV. Also, measurements of V_o and V_K have to be performed simultaneously to prevent errors due to temporal variations of V_o during the experiment. The technique employed in this study, using two separate single-barreled microelectrodes, is made possible by the syncytial character of the frog skin epithelium. As shown in Fig. 3, V_o responds identically (within 2 mV) to changes in solution composition when recorded in two different cells. There is not, however, complete synchronization of all the cells, as shown in Figs. 3, 6 and 7. In spite of the homogeneous arrangement of the mucosal perfusion inlets and the fast perfusion rate, cells in the center of the exposed area of epithelium respond faster than those in the periphery. Thus, by locating the microelectrode either in the center or in the periphery of the epithelium we could record changes in V_o faster or slower than the concomitant changes in I_t, which is an average of the current across all cells. Although in principle recording of V_o and V_K in the same cell seems a better approach, in our hands impalements of frog skin with double barreled microelectrodes have been unsatisfactory so far.

The values of a^c_K measured in this study are lower than those (132 mM) reported by Nagel et al. (1981). In that study a^c_K was determined by successive impalements with open-tip and K-selective microelectrodes, and thus estimates of a^c_K were less accurate. Recently, DeLong and Civan (1983) have measured a^c_K in split skins impaled from the basolateral side, using techniques otherwise similar to those employed here. At face value their estimate of a^c_K (93 mM), before a theoretical correction of 2.3

mV for the junction potential of 3 M KCl filled microelectrodes, agrees with ours.[4] However, these authors used the Nicolsky equation to calculate a_K^c. As explained before (Material and Methods; *see also* Edelman et al., 1978; Armstrong & García-Díaz, 1980), K microelectrodes do not exhibit a constant selectivity coefficient and the use of the Nicolsky equation overestimates a_K^c by 15 to 26 mM. The experiments where the cell was depolarized with high serosa K (Fig. 8 and Table 4) support our values of a_K^c. Under these conditions one expects from the measured a_K^c of 92 mM an E_i of about 2 mV, since any contribution to E_i from a rheogenic pump (I_p/g_i) will be greatly diminished due to the large increase in basolateral conductance. The measured values of E_i under these conditions (Table 4) are in good agreement with this expectation.

No relation was found in this study between the cell short-circuit current and a_K^c in different skins. In fact a_K^c remained fairly constant in spite of the wide range of I_c encountered (5 to 70 μA/cm^2). This is at odds with a recent report (Harvey & Kernan, 1984) where the authors found that skins with low I_c (<14 μA/cm^2) had higher a_K^c (74 mM) than those with higher I_c (a_K^c = 45 mM). We do not know the reasons for this discrepancy, but as shown below, theoretical considerations suggest a change of only 6 mM in a_K^c when I_c is abolished. Also, Rick et al. (1981, 1984) have found that the K concentration measured with the electron microprobe in frog skins increases by $\leq$12 mM after inhibition of cell current. Thus it is difficult to understand how a_K^c will change as dramatically as Harvey and Kernan (1984) found for such relatively small variations in I_c.

Inhibition of cell current by either addition of amiloride or substitution of apical Na hardly affected a_K^c (Tables 2 and 3). In some experiments a small increase in a_K^c was observed, but on the average the change was not significant. Two factors contribute to these observations. The expected change in a_K^c is a small increase, as shown by both the analysis below and electron probe measurements of the K concentration, C_K, in frog skin under the same conditions (Rick et al., 1981, 1984). Depending on the cell layer examined, these authors found that C_K either remained constant or increased up to 12 mmol/kg wet wt after amiloride addition or removal of apical Na. These changes fall within the detection limit of our technique. As mentioned before, in the range 0.1 M activity the difference $V_K - V_o$ changes by about 1 mV for every 4 mM change in a_K^c. The resolution limit of these measurements is usually 2 to 3 mV, i.e., about 8 to 12 mM change in a_K^c.

Immediately after inhibition of cell current, V_i ($=-V_o$) averages 109 mV (Tables 2 and 3). Since E_K is about 98 mV (Table 2), the passive K flux is directed inwards during the 5–10 min that V_i remains higher than E_K [*see* Fig. 6 and Eq. (3)]. But this is a transient state and thus there is no need to invoke any active extrusion of K as previously suggested (Helman et al., 1979). Calculation of the amount of K entering the cell during this reversal of the passive K flux indicates that a_K^c will increase by only 6 mM (*see* below). Of particular interest is the observation that, at the steady state after inhibition of cell current, V_i ($=E_i^x$) is lower than E_K by some 10 mV. If there is still a significant K conductance at the basolateral membrane under these conditions, K will leak out of the cell. To explain the constancy of a_K^c (*see also* Rick et al., 1981, 1984), one has to postulate that the mechanism for active K uptake is still functioning in the absence of net cellular Na transport. There are several possibilities to explain this observation. One is that the active pump mechanism has now a different stoichiometry, pumping K into the cell without any exchange for intracellular Na. Other possibilities are that Na enters the cell at the basolateral membrane, either through a small electrodiffusive leak, by Na exchange for cell Ca (Grinstein & Erlij, 1978; Taylor & Windhager, 1979; Chase & Al-Awqati, 1981), or together with Cl in an electroneutral fashion (Cox & Helman, 1983; Giráldez & Ferreira, 1984). Thus the pump could still exchange cell Na for K with the same stoichiometry of 3/2.

If, immediately after inhibition of cell current (I_c = 0), the Na-K pump is still operating in its normal mode ($I_p > 0$), from Eq. (5) we obtain $I_K = -I_p$, i.e., the passive K leak will be directed inwards and a_K^c will increase. We can estimate the increase in a_K^c from the equation:

$$\Delta a_K^c = \gamma \cdot \Delta C_K^c = -\frac{\gamma}{h} \int J_K \, dt \qquad (6)$$

where γ is the activity coefficient of K in the cytoplasm, h is the effective "cell height" (including all the layers) and J_K is the total K flux across the basolateral membrane. If, in agreement with the results shown before, the pump stoichiometry is 3Na/2K, J_K is given by

[4] DeLong and Civan (1983) corrected their values of V_o (and a_K^c) twice. The second correction tries to account for the change in junction potential at the tip of a 3 M KCl filled microelectrode when it is advanced from the Ringer's solution into the intracellular space. This calculation used the Henderson equation and estimates of intracellular electrolytes. However, the validity of the Henderson equation is questionable when applied to the submicron geometry of a microelectrode tip.

$$\mathcal{F}J_K = I_K^d - 2I_p \quad (7)$$

where I_K^d and I_p are the passive K current and pump current, respectively. When $I_c = 0$ we get from Eq. (5) $I_K^d = -I_p$. Thus

$$J_K = \frac{3}{\mathcal{F}} I_K^d. \quad (8)$$

From Eqs. (6), (8) and (3) we obtain

$$\Delta a_K^c = \frac{3\gamma g_i}{\mathcal{F}h} \int (V_i - E_K)\, dt. \quad (9)$$

Taking γ as 0.77, $h = 45$ μm (Rick et al., 1984) and assuming that g_i remains constant after inhibition of I_c, we can estimate Δa_K^c by integrating $(V_i - E_K)$ during the period that $V_i > E_K$. For the experiments shown in Table 2 Δa_K^c amounts to 6 ± 3 mM. This increase in a_K^c is of the same magnitude as the decrease in cell Na activity (4 to 8 mM) that we have observed under the same conditions in some preliminary experiments. It also agrees with the observations of Rick et al. (1981, 1984) mentioned above.[5]

Passive K and Pump Currents

The experiments shown in Table 2 allowed us to calculate the fraction of basolateral current carried by electrodiffusive movement of K, I_K^d. The basic assumption in this calculation is that essentially all of the basolateral conductance is K conductance, so that the pump virtually operates as a constant current generator. Although this is often assumed to be the case (*see*, e.g., Lindemann, 1977; Nagel, 1980), it is still a matter of speculation. The calculation of g_i from the ratio $I_c/(E_i^{max} - V_i)$, i.e., $\Delta I_c/\Delta V_o$ after a fully inhibiting dose of amiloride,is justified by experiments indicating that g_i is voltage independent (*unpublished results; see also* Fig. 7 in Nagel et al., 1983*a*). In these experiments it was found that when I_c was altered by serially clamping V_t, I_c and V_i were linearly related over the range of V_i studied (20 to 105 mV). For each skin in Table 2 the pump current, I_p, could then be estimated as $I_c - I_K$. As shown by Fig. 9, there was a significant correlation between I_p and I_c over the range of spontaneous short-circuit I_c observed (5 to 70 μA/cm^2). The slope of the regression line, 0.31, is not significantly different from the expected slope, 0.33, for a pump stoichiometry of 3Na/2K. A rheogenic pump mechanism for frog skin has also been proposed by Nagel (1980). In the absence of reliable values of E_K, this author estimated I_p as $g_i(E_i^{max} - E_i^{\infty})$. Since, as shown in Table 2, $E_i^{\infty} < E_K$, his estimates of I_p are slightly higher that the ones that would be obtained using our approach.

In conclusion, our results are consistent with the concept of a rheogenic Na-K pump with a stoichiometry of 3Na/2K and, indirectly, the notion that the pump is virtually a constant current generator. However, the above treatment is over-simplified; additional mechanisms must be invoked in order to explain the disequilibrium of K in the absence of current flow, as well as the disequilibrium of Cl noted earlier (Nagel et al., 1981; Giráldez & Ferreira, 1984). Experiments monitoring cell Na and Cl activity will be required in order to characterize the nature of the pump function and basolateral membrane conductance under a variety of experimental conditions.

This work was supported by National Institutes of Health Grant AM 29968, by U.S. Public Health Services Training Grant T32 AM 7053 (L.M.B.) and a Cystic Fibrosis Foundation Research Fellowship (G.K.).

[5] If, as mentioned before, some other mechanism(s) of ion transport is operative at the basolateral membrane, Eq. (5) must be modified accordingly.

References

Armstrong, W.McD., García-Díaz, J.F. 1980. Ion-selective microelectrodes: Theory and technique. *Fed. Proc.* **39:**2851–2859

Armstrong, W.McD., García-Díaz, J.F. 1981. Criteria for the use of microelectrodes to measure membrane potentials in epithelial cells. *In:* Epithelial Ion and Water Transport. A.D.C. MacKnight and J.P. Leader, editors. pp. 43–53. Raven Press, New York

Baxendale, L.M., García-Díaz, J.F., Essig, A. 1984. Cell potassium activity in frog skin epithelium: Response to voltage clamping and inhibition of sodium transport. *J. Gen. Physiol.* **84:**27*a*

Blatt, M.R., Slayman, C.L. 1983. KCl leakage from microelectrodes and its impact on the membrane parameters of a nonexcitable cell. *J. Membrane Biol.* **72:**223–234

Chase, H.S., Al-Awqati, Q. 1981. Regulation of the sodium permeability of the luminal border of toad bladder by intracellular sodium and calcium: Role of sodium-calcium exchange in the basolateral membrane. *J. Gen. Physiol.* **77:**693–712

Cox, T.C., Helman, S.I. 1983. Effects of ouabain and furosemide on basolateral membrane Na efflux of frog skin. *Am. J. Physiol.* **245:***F*312–*F*321

DeLong, J., Civan, M.M. 1983. Microelectrode study of K^+ accumulation by tight epithelia: I. Baseline values of split frog skin and toad urinary bladder. *J. Membrane Biol.* **72:**183–193

Edelman, A., Curci, S., Samaržija, I., Frömter, E. 1978. Determination of intracellular K activity in rat kidney proximal tubular cells. *Pfluegers Arch.* **378:**37–45

Fisher, R.S., Helman, S.I. 1981. Influence of basolateral [K] on the electrical parameters of the cells of isolated epithelia of frog skin. *Biophys. J.* **33:**41*a*

Fromm, M., Schultz, S.G. 1981. Some properties of KCl-filled

microelectrodes: Correlation of potassium "leakage" with tip resistance. *J. Membrane Biol.* **62:**239–244

Fuchs, W., Larsen, E.H., Lindemann, B. 1977. Current-voltage curve of sodium channels and concentration dependence of sodium permeability in frog skin. *J. Physiol. (London)* **267:**137–166

Giráldez, F., Ferreira, K.T.G. 1984. Intracellular chloride activity and membrane potential in stripped frog skin (*Rana temporaria*). *Biochim. Biophys. Acta* **769:**625–628

Grinstein, S., Erlij, D. 1978. Intracellular calcium and the regulation of sodium transport in the frog skin. *Proc. R. Soc. London B* **202:**353–360

Harvey, B.J., Kernan, R.P. 1984. Intracellular ion activities in frog skin in relation to external sodium and effects of amiloride and/or ouabain. *J. Physiol. (London)* **349:**501–517

Helman, S.I., Fisher, R.S. 1977. Microelectrode studies of the active Na transport pathway of frog skin. *J. Gen. Physiol.* **69:**571–604

Helman, S.I., Nagel, W., Fisher, R.S. 1979. Ouabain on active transepithelial sodium transport in frog skin: Studies with microelectrodes. *J. Gen. Physiol.* **74:**105–127

Helman, S.I., Thompson, S.M. 1982. Interpretation and use of electrical equivalent circuits in studies of epithelial tissues. *Am. J. Physiol.* **243:***F*519–*F*531

Koefoed-Johnsen, V., Ussing, H.H. 1958. The nature of the frog skin potential. *Acta Physiol. Scand.* **42:**298–308

Kristensen, P. 1983. Exchange diffusion, electrodiffusion, and rectification in the chloride transport pathway of frog skin. *J. Membrane Biol.* **72:**141–151

Lindemann, B. 1977. Circuit analysis of epithelial ion transport: I. Derivation of network equations. *Bioelectrochem. Bioenerg.* **4:**287–297

Nagel, W. 1976. The intracellular electrical profile of the frog skin epithelium. *Pfluegers Arch.* **365:**135–143

Nagel, W. 1979. Inhibition of potassium conductance by barium in frog skin epithelium. *Biochim. Biophys. Acta* **552:**346–357

Nagel, W. 1980. Rheogenic sodium transport in a tight epithelium, the amphibian skin. *J. Physiol. (London)* **302:**281–295

Nagel, W., García-Díaz, J.F., Armstrong, W.McD. 1981. Intracellular ionic activities in frog skin. *J. Membrane Biol.* **61:**127–134

Nagel, W., García-Díaz, J.F., Essig, A. 1983*a*. Cellular and paracellular conductance patterns in voltage-clamped frog skin. *In:* Membrane Biophysics: II. Physical Methods in the Study of Epithelia. M.A. Dinno, A.B. Callahan, and T.C. Rozzell, editors. pp. 221–231. Alan R. Liss, New York

Nagel, W., García-Díaz, J.F., Essig, A. 1983*b*. Contribution of junctional conductance to the cellular voltage-divider ratio in frog skins. *Pfluegers Arch.* **399:**336–341

Nagel, W., García-Díaz, J.F., Essig, A. 1983*c*. Effect of voltage perturbation on transcellular sodium transport of frog skin. Falk Symposium: Intestinal Absorption and Secretion. Titisee, June 2–4

Nelson, D.J., Ehrenfeld, J., Lindemann, B. 1978. Volume changes and potential artifacts of epithelial cells of frog skin following impalement with microelectrodes filled with 3 M KCl. *J. Membrane Biol.* **Special Issue:**91–119

Nielsen, R. 1984. Active transepithelial potassium transport in frog skin via specific potassium channels in the apical membrane. *Acta Physiol. Scand.* **120:**287–296

Rick, R., Dorge, A., Thurau, K. 1981. Electron microprobe analysis of frog skin epithelium: Pathway of transepithelial sodium transport. *In:* Ion Transport by Epithelia. S.G. Schultz, editor. pp. 197–208. Raven, New York

Rick, R., Roloff, C., Dörge, A., Beck, F.X., Thurau, K. 1984. Intracellular electrolyte concentrations in the frog skin epithelium: Effect of vasopressin and dependence on the Na concentration in the bathing media. *J. Membrane Biol.* **78:**129–145

Singer, I., Civan, M. 1971. Effects of anions on sodium transport in toad urinary bladder. *Am. J. Physiol.* **221:**1019–1026

Stoner, L.C., Natke, E., Jr., Dixon, M.K. 1984. Direct measurement of potassium leak from single 3 M KCl microelectrodes. *Am. J. Physiol.* **246:***F*343–*F*348

Taylor, A., Windhager, E.E. 1979. Possible role of cytosolic calcium and Na-Ca exchange in regulation of transepithelial sodium transport. *Am. J. Physiol.* **236:***F*505–*F*512

Thompson, I.G., Mills, J.W. 1983. Chloride transport in glands of frog skin. *Am. J. Physiol.* **244:***C*221–*C*226

Turnheim, K., Frizzell, R.A., Schultz, S.G. 1977. Effect of anions on amiloride-sensitive, active sodium transport across rabbit colon, *in vitro:* Evidence for *trans*-inhibition of the Na entry mechanism. *J. Membrane Biol.* **37:**63–84

Ussing, H.H., Biber, T.U.L., Bricker, N.S. 1965. Exposure of the isolated frog skin to high potassium concentrations at the internal surface: II. Changes in epithelial cell volume, resistance and response to antidiuretic hormone. *J. Gen. Physiol.* **48:**425–433

Received 11 September 1984